Resonant Phase Matching of Josephson Junction Traveling Wave Parametric Amplifiers

Kevin O'Brien,[1] Chris Macklin,[2] Irfan Siddiqi,[2] and Xiang Zhang[1,3,*]

[1]*Nanoscale Science and Engineering Center, University of California, Berkeley, California 94720, USA*
[2]*Department of Physics, University of California, Quantum Nanoelectronics Laboratory, Berkeley, California 94720, USA*
[3]*Materials Sciences Division, Lawrence Berkeley National Laboratory, Berkeley, California 94720, USA*

We propose a technique to overcome phase mismatch in Josephson-junction traveling wave parametric amplifiers in order to achieve high gain over a broad bandwidth. Using "resonant phase matching," we design a compact superconducting device consisting of a transmission line with subwavelength resonant inclusions that simultaneously achieves a gain of 20 dB, an instantaneous bandwidth of 3 GHz, and a saturation power of −98 dBm. Such an amplifier is well suited to cryogenic broadband microwave measurements such as the multiplexed readout of quantum coherent circuits based on superconducting, semiconducting, or nanomechanical elements, as well as traditional astronomical detectors.

PACS numbers: 85.25.-j, 42.65.Yj, 74.81.Fa, 84.30.Le

Josephson parametric amplifiers [1–5] routinely approach quantum-noise-limited performance [6–9] and are currently used in sensitive experiments requiring high-fidelity detection of single-photon-level microwave signals, such as the readout and feedback control of superconducting quantum bits [10–17], and magnetometry with the promise of single-spin resolution [3]. To obtain a large parametric gain, the interaction time with the material nonlinearity—the order-unity nonlinear inductance of the Josephson junction—must be maximized. Current Josephson parametric devices increase the interaction time by coupling the junction to a resonant cavity, albeit at the expense of instantaneous bandwidth. In contrast, traveling wave parametric amplifiers (TWPAs) [18–21] achieve long interaction times by utilizing long propagation lengths rather than employing multiple bounces in a cavity, thereby avoiding the inherent gain-bandwidth trade-off associated with cavity based devices. A major challenge in the design of TWPAs, however, is that optimum parametric gain is achieved only when the amplification process is phase matched. TWPAs based on Josephson junctions have been investigated theoretically [22–25] and experimentally [26–28] but have not demonstrated sufficient gain, in part due to phase-matching limitations, to replace existing semiconductor amplifier technology. TWPAs based on the weaker nonlinear kinetic inductance of thin titanium nitride wires and phase matched through periodic loading have also been demonstrated [29,30], but they require significantly longer propagation lengths and higher pump powers to achieve comparable gain. In this Letter, we show that by adding a resonant element into the transmission line, phase matching and exponential gain can be achieved over a broad bandwidth.

The proposed traveling wave parametric amplifier consists of a Josephson-junction-loaded transmission line [Fig. 1(a)] with a capacitively coupled parallel *LC* resonator shunt to allow phase matching. The *LC* resonator

shunt [colored red in Figs. 1(a) and 1(b)] creates a stop band [Fig. 1(c), red line] in the otherwise approximately linear dispersion relation [Fig. 1(c), black dashed line]. In the presence of a strong copropagating pump wave, a weak signal propagating in the TWPA is amplified through a four wave mixing interaction. Four wave mixing in the weak pump limit is perfectly phase matched for a linear dispersion; however, a strong pump modifies the phase velocities through self- and cross phase modulation, generating a phase mismatch and preventing exponential gain. We compensate for this phase mismatch by tuning the pump frequency near the pole of the *LC* resonator. In a dissipationless system such as a superconducting circuit, a resonant element opens a stop band [inset of Fig. 1(c)] in which the wave vector is purely imaginary, surrounded by regions in which the wave vector is purely real and varies from 0 to π/a, where a is the size of the unit cell. The wave vector of the pump can be set to arbitrary values by varying the frequency with respect to the resonance in order to eliminate the phase mismatch.

We now calculate the value of the phase mismatch and the expected device performance when phase matching is achieved. We use a first principles model for the nonlinear dynamics in the Josephson-junction transmission line [24,25], which has been validated by experiments [28]. By making the ansatz that the solutions are traveling waves, taking the slowly varying envelope approximation, and neglecting pump depletion, we obtain a set of coupled wave equations which describe the energy exchange between the pump, the signal, and the idler in the undepleted pump approximation (see Supplemental Material [31] for the derivation):

$$\frac{\partial a_s}{\partial x} - i\kappa_s a_i^* e^{i(\Delta k_L + 2\alpha_p - \alpha_s - \alpha_i)x} = 0, \qquad (1)$$

$$\frac{\partial a_i}{\partial x} - i\kappa_i a_s^* e^{i(\Delta k_L + 2\alpha_p - \alpha_s - \alpha_i)x} = 0, \qquad (2)$$
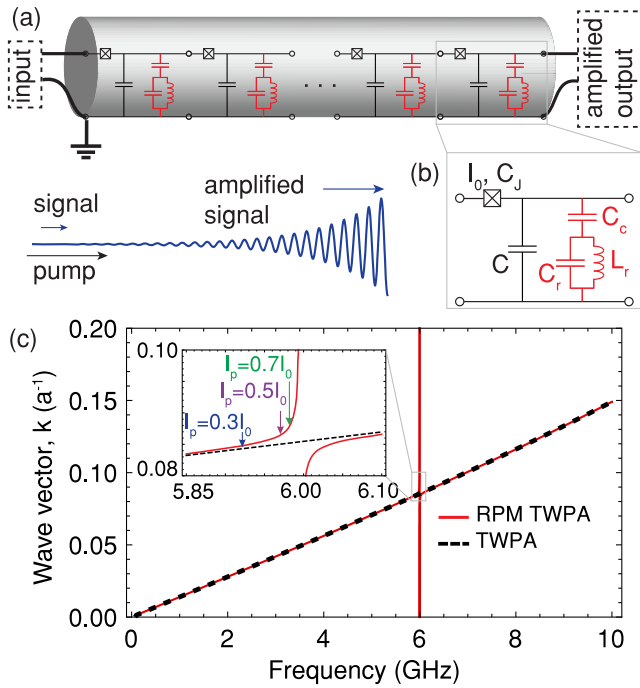
FIG. 1 (color online). Resonantly phase-matched traveling wave parametric amplifier. (a) Signal photons are amplified through a nonlinear interaction with a strong pump as they propagate along the 2000 unit cell transmission line with a lattice period of $a = 10\ \mu m$. (b) In each unit cell a Josephson junction, a nonlinear inductor, is capacitively coupled to an LC resonator. The circuit parameters are $C_j = 329\ fF$, $L = 100\ pH$, $C = 39\ fF$, $C_c = 10\ fF$, $C_r = 7.036\ pF$, $L_r = 100\ pH$, $I_0 = 3.29\ \mu A$. (c) The LC circuit opens a stop band (red line) in the dispersion relation of the TWPA (black dashed line) whose frequency depends on the circuit parameters. In the inset, we plot the pump frequency to phase match a pump current of $0.3I_0$ (blue), $0.5I_0$ (purple), and $0.7I_0$ (green), where I_0 is the junction critical current.

where a_s and a_i are the signal and idler amplitudes, $\Delta k_L = 2k_p - k_s - k_i$ is the phase mismatch in the low pump power limit, and the coupling factors α_p, α_s, and α_i represent the change in the wave vector of the pump, the signal, and the idler due to self- and cross phase modulation induced by the pump. The coupling factors depend on the circuit parameters (see Eqs. (15), (16), and (17) in the Supplemental Material [31]) and scale quadratically with the pump current. Maximum parametric gain is achieved when the exponential terms are constant: the phase mismatch, $\Delta k = \Delta k_L + 2\alpha_p - \alpha_s - \alpha_i$, must then be zero. The coupled wave equations (1) and (2) are similar to the coupled amplitude equations for an optical parametric amplifier [32] and have the solution

$$a_s(x) = a_s(0)\left(\cosh gx - \frac{i\Delta k}{2g}\sinh gx\right)e^{i\Delta kx/2} \quad (3)$$

with the gain coefficient $g = \sqrt{\kappa_s \kappa_i^* - (\Delta k/2)^2}$. For zero initial idler amplitude and perfect phase matching, this leads to exponential gain, $a_s(x) \approx a_s(0)e^{gx}/2$. For poor phase

matching, g is imaginary and the gain scales quadratically with length rather than exponentially.

Without resonant phase matching, the parametric amplification is phase matched at zero pump power, but rapidly loses phase matching as the pump power increases. Neglecting dispersion and frequency dependent impedances, the exact expression for the phase mismatch can be simplified to yield $\Delta k \approx 2k_p - k_s - k_i - 2k_p\kappa$, where $\kappa = (a^2 k_p^2 |Z_{\text{char}}|^2 / 16L^2\omega_p^2)(I_p/I_0)^2$. The nonlinear process creates a pump power dependent phase mismatch which can be compensated for by increasing the pump wave vector.

In Fig. 2, we show the increase in gain due to resonant phase matching for the device described in Fig 1. Resonant phase matching increases the gain by more than one order of magnitude from 10 dB to 21 dB [Fig. 2(a)] for a pump current of half the junction critical current and a pump frequency, 5.97 GHz, on the lower frequency tail of the resonance, as shown in the inset of Fig. 1(c). The increase in the pump wave vector due to the resonance compensates for the phase mismatch from cross and self-phase modulation [Fig. 2(b), black dashed line], leading to perfect phase matching near the pump frequency [Fig. 2(b), purple]. For higher pump currents, the benefits are even more pronounced: the RPM (resonantly phase matched) TWPA achieves 50 dB of gain (compared to 15 dB for the TWPA) with a pump current of $0.7I_0$ [Fig. 2(c)]. Achieving 50 dB of gain over a 3 GHz bandwidth would require a larger junction critical current than used here to prevent gain saturation by vacuum photons. By varying the pump frequency relative to the resonance, the parametric amplification can be phase matched for arbitrary pump currents [Fig. 2(d)]. Due to this ability to tune the pump phase mismatch over the entire range of possible wave vectors, this technique is highly flexible.

We now examine the scaling relations for the gain in order to obtain the optimum gain through engineering the linear and nonlinear properties of the transmission line. Simplifying the expression for the gain by assuming perfect phase matching and neglecting the effects of the resonant element and the junction resonance on the dispersion, we find that the exponential gain coefficient is directly proportional to the wave vector $g \propto k_p I_p^2/I_0^2$. See the Supplemental Material [31] for full expressions for the wave vector, characteristic impedance, and the gain with parameter variations using stochastic calculus [33]. Thus, for a fixed pump strength relative to the junction critical current, the gain coefficient is proportional to the electrical length. In other words, a larger wave vector and thus slower light leads to a larger effective nonlinearity due to the higher energy density; this effect is well known in photonic crystals [34]. For convenient integration with commercial electronics, the characteristic impedance is designed to be $Z_{\text{char}} \approx \sqrt{L/(C + C_c)} \approx 50\ \Omega$, which fixes the ratio of the inductance and the capacitance. The wave vector is
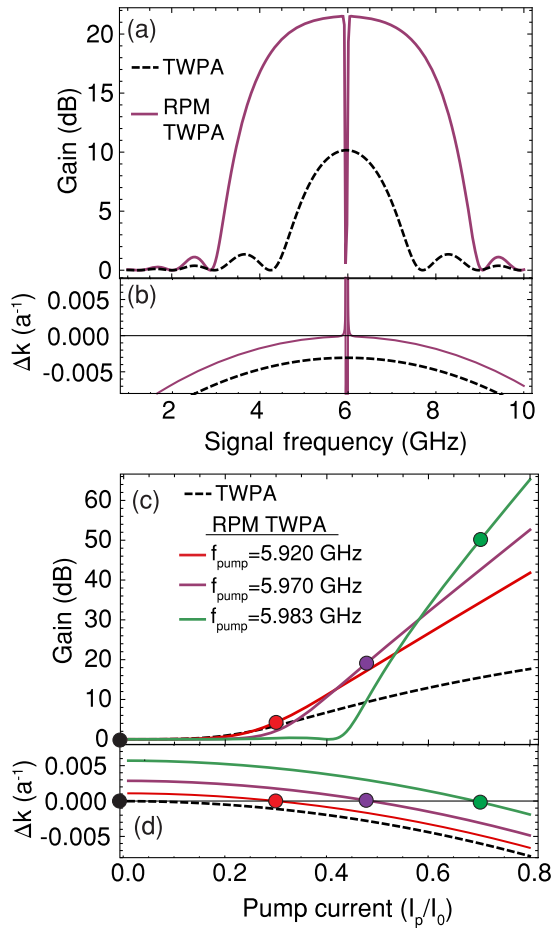
FIG. 2 (color online). Gain of the RPM TWPA. (a) The gain as a function of signal frequency in dB with RPM (purple line) and without (black dashed line) for a pump current of $0.5I_0$ and a pump frequency of 5.97 GHz. (b) The phase mismatch with (purple line) and without (black dashed line) RPM. (c) The peak gain as a function of pump current without RPM (black dashed line) and with RPM for three different pump frequencies, which phase match the parametric amplification for pump currents of $0.3I_0$ (red line), $0.5I_0$ (purple line), and $0.7I_0$ (green line). (d) The phase mismatch as a function of pump current. The dots mark the pump current where the parametric amplification is perfectly phase matched.

proportional to the product of the capacitance and the inductance $k \approx \omega/a\sqrt{L(C+C_c)}$. Increasing both the capacitance and the inductance or decreasing the unit cell size are effective strategies for increasing the gain per unit length while maintaining impedance matching for a 50 ohm load. The current design represents a trade-off between unit cell size and component values which is convenient to fabricate.

Next we consider the dynamic range of the amplifier. The upper limit of the dynamic range is due to pump depletion: the pump transfers energy to the signal and the idler, which reduces the parametric gain. To investigate this regime, we solve for the coupled wave equations without

the undepleted pump approximation, resulting in four coupled nonlinear differential equations (Eqs. (43)–(46) in the Supplemental Material [31]), which are solved by transforming them to real differential equations and expressing them as a Jacobi elliptic integral [35]. The gain as a function of input signal power calculated including pump depletion (solid lines in Fig. 3) is in excellent agreement with the approximate yet general solution for pump depletion (dashed lines in Fig. 3) in a four photon parametric amplifier [36]:

$$G = \frac{G_0}{1 + 2G_0 I_s^2/I_p^2},\qquad(4)$$

where G_0 is the small signal gain in linear units and I_s and I_p are the input signal and pump currents. From Eq. (4), the gain compression point is approximately $P_{1\,\text{dB}} = P_p/(2G_0)$. Thus, the threshold for gain saturation is independent of the specific device configuration and depends only on the small signal gain and the pump power. The
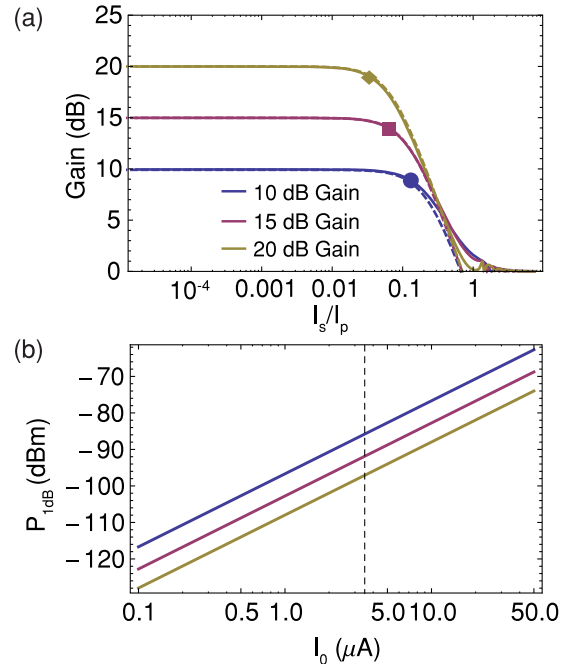

FIG. 3 (color online). Effect of pump depletion on dynamic range. (a) The gain as a function of input signal current (normalized to the pump current) for a small signal gain of 10, 15, and 20 dB obtained with a pump current of $0.5I_0$ and device lengths of 1150, 1530, and 1900 unit cells. The approximation for the gain depletion (dashed lines) from Eq. (4) is in excellent agreement with the result obtained by solving the full nonlinear dynamics (solid lines). (b) $P_{1\,\text{dB}}$, the input signal power where the gain decreases by 1 dB, as a function of junction critical current I_0 with the pump current fixed at $0.5I_0$. The black dashed line corresponds to the device considered in this Letter, which has a gain compression point of $P_{1\,\text{dB}} = -87$, -93, and -98 dBm, for a gain of 10, 15, and 20 dB for a junction critical current of $I_0 = 3.29$ μA.

gain as a function of input signal current is plotted for three values of the small signal gain in Fig. 3(a). The signal current at which the gain drops by 1 dB is marked on the curves of Fig. 3(a). With a pump current of $0.5I_0$, the signal power where the gain decreases by 1 dB is -87, -93, and -98 dBm, for a small signal gain of 10, 15, and 20 dB, respectively. These gain compression points are consistent with the approximate relation with the pump power of -69 dBm. The dynamic range of the TWPA is significantly higher than a cavity based Josephson parametric amplifier with the same junction critical current since the lack of a cavity enables a higher pump current before the Josephson junction is saturated.

To further increase the threshold for gain saturation, the junction critical current can be scaled up, as seen in Fig. 3(b). However, increasing the junction critical current decreases the inductance, which reduces the wave vector, leading to a weaker nonlinearity. One potential solution is to use N Josephson junctions, each with a critical current I_0/N in a series as a superinductor [37]. The 1 dB power then scales as $\sqrt{N}$, leading to a larger dynamic range at the expense of a more complex fabrication.

We now estimate the potential for third or higher harmonic generation, which would cause pump depletion and distortion through self steepening [38,39]. From the coupled wave equations describing third harmonic generation, we find that the third harmonic is poorly phase matched and less than 0.1% of the pump is converted to the third harmonic (Eq. (41) and Fig. 1 in the Supplemental Material [31]).

Resonant phase matching has an important advantage over dispersion engineering through periodic loading, which has been used to phase match TWPAs based on the weaker nonlinear kinetic inductance [29,30]. A disadvantage of periodic loading is the potential phase matching of backward parametric amplification. Dispersion engineering through periodic loading opens a photonic band gap (Fig. 4) near the pump frequency and through band bending changes the pump wave propagation constant to phase match forward parametric amplification. Periodic loading creates an effective momentum inversely proportional to the periodicity of the loading $G = 2\pi/\Lambda$, where Λ is the periodicity of the loading and G is the reciprocal lattice vector. The periodicity is chosen so that the stop band is at $G/2 \approx k_p$. In such a periodic system, the phase matching relation needs only to be satisfied up to an integer multiple of the reciprocal lattice vector [40]. As can be seen from the phase-matching relation, the effective momentum from the lattice phase matches the parametric amplification process for a backward propagating signal $\Delta k_{L,b} = 2k_p + k_s + k_i + nG \approx 0$ for $n = -2$. Under this condition, any backward propagating photons present in the system will be amplified, leading to gain ripples and a reduced threshold for parametric oscillations. Due to imperfect impedance matching over the operating band of the amplifier, a weak standing wave
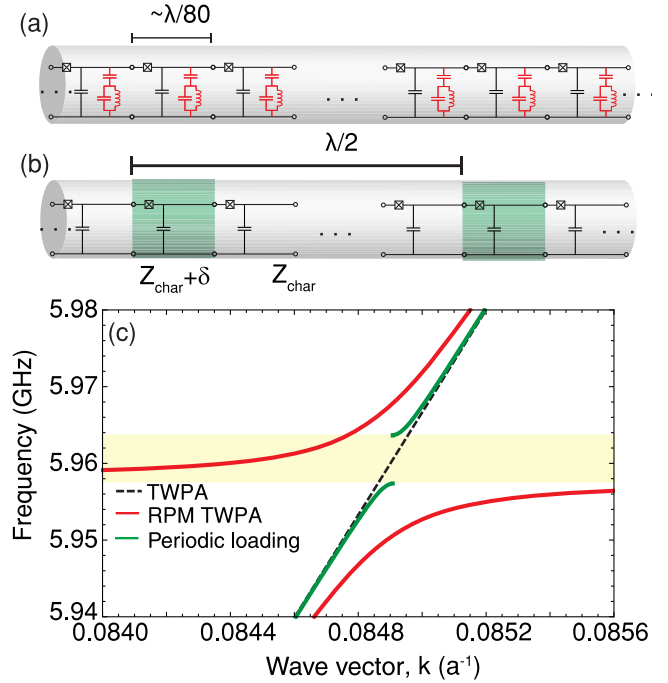

FIG. 4 (color online). Band structure of resonantly phase matched and periodically loaded TWPAs. The parametric amplifier without a resonant element [(a), black only], with a resonant element [(a), black and red], and with periodic loading (b): every 37th unit cell has a slightly different capacitance and inductance (green). (c) The wave vector as a function of frequency for the TWPA (black dashed line), RPM TWPA (red line), and TWPA with periodic loading (green lines). The yellow shaded region indicates the photonic band gap due to the periodic loading. The main difference between the photonic band gap and the resonator is the edge of the Brillouin zone. For the resonant element, the zone boundary is at π/a, while the other periodically loaded transmission line has zone boundary at $\pi/(37a)$, which is determined by the period of the loading. The effective momentum due to the periodic loading is close to k_p, which may phase match backward parametric amplification.

condition will be set up in the nonlinear transmission line due to the return loss at the output and the input. If the return loss in dB is R, then the magnitude of the standing signal will be of order $2R$. However, the signal experiences some gain (in dB) in the forward and reverse directions, G_f and G_r. If $G_f + G_r + 2R$ approaches unity, the device becomes a parametric oscillator. The proposed resonant phase matching technique phase matches only the forward parametric amplification process, so the maximum gain before the onset of parametric oscillations may be higher than in a device utilizing periodic loading.

In conclusion, we have proposed a traveling wave parametric amplifier which is phase matched by subwavelength resonant elements in order to achieve 20 dB of gain, 3 GHz of bandwidth, and a saturation power ($P_{1\,dB}$) of -98 dBm. This device will be well suited to multiplexed readout of quantum bits and astronomical detectors.

Applying metamaterial design techniques to nonlinear superconducting systems may yield a number of useful devices for circuit quantum electrodynamics, such as backward parametric amplifiers or mirror-less optical parametric oscillators [41].

[*]xiang@berkeley.edu

[1] M. A. Castellanos-Beltran and K. W. Lehnert, Appl. Phys. Lett. **91**, 083509 (2007).

[2] N. Bergeal, F. Schackert, M. Metcalfe, R. Vijay, V. E. Manucharyan, L. Frunzio, D. E. Prober, R. J. Schoelkopf, S. M. Girvin, and M. H. Devoret, Nature (London) **465**, 64 (2010).

[3] M. Hatridge, R. Vijay, D. H. Slichter, J. Clarke, and I. Siddiqi, Phys. Rev. B **83**, 134501 (2011).

[4] N. Roch, E. Flurin, F. Nguyen, P. Morfin, P. Campagne-Ibarcq, M. H. Devoret, and B. Huard, Phys. Rev. Lett. **108**, 147701 (2012).

[5] C. Eichler, Y. Salathe, J. Mlynek, S. Schmidt, and A. Wallraff, arXiv:1404.4643.

[6] W. H. Louisell, A. Yariv, and A. E. Siegman, Phys. Rev. **124**, 1646 (1961).

[7] E. M. Levenson-Falk, R. Vijay, N. Antler, and I. Siddiqi, Supercond. Sci. Technol. **26**, 055015 (2013).

[8] M. A. Castellanos-Beltran, K. D. Irwin, G. C. Hilton, L. R. Vale, and K. W. Lehnert, Nat. Phys. **4**, 929 (2008).

[9] F. Mallet, M. A. Castellanos-Beltran, H. S. Ku, S. Glancy, E. Knill, K. D. Irwin, G. C. Hilton, L. R. Vale, and K. W. Lehnert, Phys. Rev. Lett. **106**, 220502 (2011).

[10] K. W. Murch, S. J. Weber, C. Macklin, and I. Siddiqi, Nature (London) **502**, 211 (2013).

[11] R. Vijay, C. Macklin, D. H. Slichter, S. J. Weber, K. W. Murch, R. Naik, A. N. Korotkov, and I. Siddiqi, Nature (London) **490**, 77 (2012).

[12] J. E. Johnson, C. Macklin, D. H. Slichter, R. Vijay, E. B. Weingarten, J. Clarke, and I. Siddiqi, Phys. Rev. Lett. **109**, 050506 (2012).

[13] R. Vijay, D. H. Slichter, and I. Siddiqi, Phys. Rev. Lett. **106**, 110502 (2011).

[14] M. Hatridge, S. Shankar, M. Mirrahimi, F. Schackert, K. Geerlings, T. Brecht, K. M. Sliwa, B. Abdo, L. Frunzio, S. M. Girvin, R. J. Schoelkopf, and M. H. Devoret, Science **339**, 178 (2013).

[15] P. Campagne-Ibarcq, E. Flurin, N. Roch, D. Darson, P. Morfin, M. Mirrahimi, M. H. Devoret, F. Mallet, and B. Huard, Phys. Rev. X **3**, 021008 (2013).

[16] D. Ristè, M. Dukalski, C. A. Watson, G. de Lange, M. J. Tiggelman, Y. M. Blanter, K. W. Lehnert, R. N. Schouten, and L. DiCarlo, Nature (London) **502**, 350 (2013).

[17] D. Ristè, J. G. van Leeuwen, H. S. Ku, K. W. Lehnert, and L. DiCarlo, Phys. Rev. Lett. **109**, 050507 (2012).

[18] A. L. Cullen, Nature (London) **181**, 332 (1958).

[19] A. L. Cullen, Proc. Inst. Electr. Eng., Part B **107**, 101 (1960).

[20] A. Sörenssen, Appl. Sci. Res., Sect. B **10**, 463 (1962).

[21] P. K. Tien, J. Appl. Phys. **29**, 1347 (1958).

[22] M. J. Feldman, P. T. Parrish, and R. Y. Chiao, J. Appl. Phys. **46**, 4031 (1975).

[23] M. Sweeny and R. Mahler, IEEE Trans. Magn. **21**, 654 (1985).

[24] O. Yaakobi, L. Friedland, C. Macklin, and I. Siddiqi, Phys. Rev. B **87**, 144301 (2013).

[25] O. Yaakobi, L. Friedland, C. Macklin, and I. Siddiqi, Phys. Rev. B **88**, 219904(E) (2013).

[26] S. Wahlsten, S. Rudner, and T. Claeson, Appl. Phys. Lett. **30**, 298 (1977).

[27] B. Yurke, M. L. Roukes, R. Movshovich, and A. N. Pargellis, Appl. Phys. Lett. **69**, 3078 (1996).

[28] C. Macklin et al. (to be published).

[29] B. Ho Eom, P. K. Day, H. G. LeDuc, and J. Zmuidzinas, Nat. Phys. **8**, 623 (2012).

[30] C. Bockstiegel, J. Gao, M. R. Vissers, M. Sandberg, S. Chaudhuri, A. Sanders, L. R. Vale, K. D. Irwin, and D. P. Pappas, J. Low Temp. Phys. **176**, 476 (2014).

[31] See Supplemental Material at http://link.aps.org/supplemental/10.1103/PhysRevLett.113.157001 for additional details, derivations, and estimated tolerance to harmonic generation and parameter variation.

[32] J. A. Armstrong, N. Bloembergen, J. Ducuing, and P. S. Pershan, Phys. Rev. **127**, 1918 (1962).

[33] M. Karlsson, J. Opt. Soc. Am. B **15**, 2269 (1998).

[34] M. Soljačić, S. G. Johnson, S. Fan, M. Ibanescu, E. Ippen, and J. D. Joannopoulos, J. Opt. Soc. Am. B **19**, 2052 (2002).

[35] Y. Chen, J. Opt. Soc. Am. B **6**, 1986 (1989).

[36] P. Kylemark, H. Sunnerud, M. Karlsson, and P. A. Andrekson, J. Lightwave Technol. **24**, 3471 (2006).

[37] N. A. Masluk, I. M. Pop, A. Kamal, Z. K. Minev, and M. H. Devoret, Phys. Rev. Lett. **109**, 137002 (2012).

[38] R. Landauer, J. Appl. Phys. **31**, 479 (1960).

[39] R. Landauer, IBM J. Res. Dev. **4**, 391 (1960).

[40] N. Bloembergen and A. J. Sievers, Appl. Phys. Lett. **17**, 483 (1970).

[41] A. K. Popov, S. A. Myslivets, and V. M. Shalaev, Opt. Lett. **34**, 1165 (2009).